技術論文

Development of Inspection and Repair Technology for the Micro Cracks on Heat Exchanger Tubes

NISHIMURA Akihiko, SHOBU Takahisa, OKA Kiyoshi, YAMAGUCHI Toshihiko
SHIMADA Yukihiro, MIHALACHE Obideu, TAGAWA Akihiro, YAMASHITA Takuya

Japan Atomic Energy Agency (8-1 Umebidai Kizugawa, Kyoto 619-0215, Japan)
nishimura.akihiko@jaea.go.jp

(Received June 22, 2010)

A prototype probe system with a hybrid optical fiber scope was designed for inspecting and re-pairing the micro cracks on heat exchanger tubes in fast breeder reactors (FBRs). It comprised a la-ser processing head combined with an eddy current testing unit. Ultrashort laser pulse ablation was used to remove work-hardened layers. And spot laser welding was used to repair the micro cracks. This system has both safe and economical options for the maintenance of FBRs because it extends the lifetime of the heat exchangers.

Key words: micro crack, heat exchanger tube, composite-type optical fiber scope, laser welding, eddy current testing, laser ablation, X-ray stress measurement

1. Introduction

At present, laser material processing is widely used to fabricate precision industrial products such as electronic devices and mechanical parts on actual industrial lines. Laser welding[1] can also be applied in the maintenance of large structures such as nuclear reactors and chemical factories. Internal access to a blanket cooling pipe with a bend section is inevitably required in Deuterium - Tritium burning reactors such as the International Thermonuclear Experimental Reactor (ITER). At the Japan Atomic Energy Agency (JAEA), an internal-access pipe welding/cutting/inspection tool for manifolds and branch pipes was developed for this purpose[2,3]. Here, the design concept of the welding/cutting/inspection processing head with a composite-type flexible optical fiber was presented for welding, cutting and close observation. This tool allowed effective inspection in observation. Then, it succeeded to cut and weld branch pipes up to 50 mm in diameter.

Laser peening has been found to be effective in maintaining nuclear reactors. The second harmonic pulses of nanosecond YAG lasers can induce compressive residual stresses at the surface layers in water. This has become an indispensable technique for better prevention of stress corrosion cracking (SCC) in reactor core shrouds and containment vessels[4]. In a more recent investigation, it was demonstrated that ultrashort laser ablation also results in good prevention of SCC in stainless stee[5]. The ablation experiments were carried out in a shield of argon gas. In this study, the hardened thin layers mechanically induced by a milling machine were successfully removed by ultra-short laser ablation without thermal damage.

In order to detect SCC or any other defects on the inner surface of heat exchanger tubes, several eddy current testing (ECT) probes have been developed[6]. At the JAEA, the ECT probe used to detect defects in helical heating tubes in the fast breeder reactor (FBR) "Monju" was specially designed and tested using a mock-up heat exchanger facility[7]. The present ECT probe is limited to the detection of cracking on the helical heating tubes. After detection, the cracks in the tubes are regularly plugged. Hence, the development of inspection and repair technologies to extend the lifetime of FBR heat exchanger units is indispensable.

This report described new related technologies to detect and repair micro cracks on heat exchanger tubes by laser ablation and welding. First, ultrashort laser ablation was tested on stainless steel for residual stress measurement in order to examine its validity. Second, the original concept, combining a composite-type optical fiberscope and a laser processing head with an ECT unit, was presented. This system was designed to repair micro cracks on welded section of heat exchanger tubes.

2. Laser ablation experiment

In previous work, ultrashort laser pulses were typically irradiated to ablate a 2-mm-square cubic sample surface[5]. The cubic sample was cut into two pieces to measure hardness distribution along the depth with a Vickers hardness tester. The following experiment used a larger area of 1 × 10 cm, where the number of scanning cycles and the laser spot diameter were tested. The area of 1 × 10 cm was equal to the circumference length of the laser-welded joint sections of FBR heat exchanger tubes.

2.1 Sample preparation and laser system

The sample material was 304L austenitic stainless steel. The chemical composition was 18.43% Cr, 9.78% Ni, 0.85% Mn, 0.58% Si and 0.009% C. After a steel plate had been annealed at 1050 ℃ for 61 minutes, a milling machine artificially repro-

duced work-hardened layers on it. Then the steel plate was cut and sliced into samples of 200 × 100 mm in size with a thickness of 5 mm. Laser ablation was carried out on the surface of each sample. A Ti:Sapphire Chirped Pulse Amplification laser (Thales Laser α10) was used. A laser pulse duration of 50 fs with pulse energy of 27 mJ was focused by a 50 mm focal length plane-concave lens on the plate in air. During laser irradiation, the sample was fixed on a holder having a 3D motion-controlled stage.

In order to apply the abovementioned laser processing for the maintenance of the heat exchanger units, it is very important to be able to access the inner walls of the heat exchanger tubes. The heat exchanger consists of an evaporator and a superheater. In the evaporator, the outer diameter of the tubes is 31.8 mm. The material used for the evaporator is steel with 2.25% chromium and a thickness of 3.8 mm. In the superheater, 3.5-mm-thick stainless steel 321 is used. The length of the evaporator is 85 m and that of the superheater is 47 m. The tube has a helical shape with a radius of 1.2–2.7 m. The minimum radius around the inlet/outlet is 0.16 m.

The relation between the scanning X-Y directions is shown in Fig. 1. One scanning cycle means that the scanning in the x-direction begins from "start" and then the scanning in the y-direction returns to "end." Each scan had a 1 mm shift at the return. One scanning cycle took 131 seconds. Table 1 shows the combination of the number of scanning cycles and the spot diameter on the sample surface. Nine laser-processed samples and one reference sample without laser processing were prepared. The spot diameter was changed from 0.3 to 0.9 mm by the Z-direction motion.

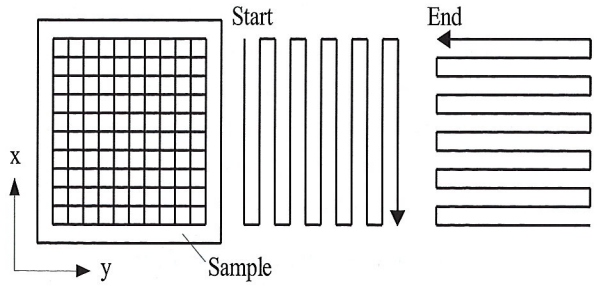

Fig. 1 Scheme of laser pulse scanning

Table 1 Conditions for laser ablation.

		Number of scanning cycles			
		0	1	3	7
Spot diameter, mm	0.3	No. 0	No. 1	No. 2	No. 3
	0.6		No. 4	No. 5	No. 6
	0.9		No. 7	No. 8	No. 9

2.2 Microscopic observations

Figure 2 shows the selected pictures of the sample surfaces, measured by an opt-ical microscope. Machining left its traces on the sample surface shown in Fig. 2(a). The picture area is 2 × 1.5 mm. The horizontally machined traces had spacing of approximately 0.6 mm. The traces were like grooves on optical gratings, which were exposed to laser irradiation.

The scheme of the laser pulse scanning created a zebra pattern. Figures 2(b) and 2(c) show the sample surfaces after laser irradiation. Each one has the area of 11 × 7 mm. In Fig. 2(b), the number of scanning cycles was 3. The characteristic zebra pattern appears in the case of a spot diameter of 0.3 mm. This was because the periodic scanning induced repetitive oxidization and ablation with deposition of oxide micro-particles. In Fig. 2(c), the number of scanning cycles was 7 with a spot diameter of 0.9 mm.

As the spot diameter increases, the zebra patterns became wider and more obscure. The depths of the initial traces gradually became shallower as the number of scanning cycles increases.

3. Design concept of a new probe system

In the evaporator, there is both boiling water and steam in the heat exchanger tubes. The transit position from water to steam depends on the operational temperature of the liquid sodium coolant. The inner surface of the tube turns into an oxide layer of magnetite that can prevent further erosion. The steam generated in the evaporator is supplied to the super-heater where it is heated under dry conditions. If even a tiny amount hot water leaks and comes into contact with liquid sodium, it could seriously damage the heat exchanger unit; this would result in immediate suspension of the power plant operation. From the perspective of risk assessment, more attention should be given to the detection of erosion symptoms in the evaporator than in the super-heater.

The prototype probe system should be able to inspect the inner wall of a 1-inch-diameter tube that is covered with a magnetite layer. Figure 3 shows the schematic view of the prototype probing system. It was designed to use a composite-type optical fiberscope, which delivers processing laser pulses and provides images of the repaired inner wall.

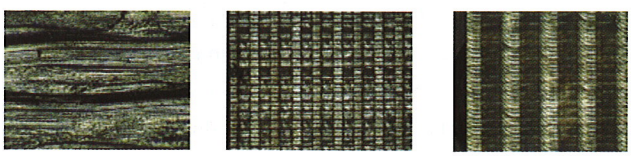

(a) No. 0 (b) No. 2 (c) No. 9

Fig. 2 Microscopic views of SUS304 sample surface

3.1 Composite-type optical fiber scope

Endoscopic techniques have been widely used in minimally-invasive abdominal surgical procedures because only a few keyhole incisions are required. The use of a composite-type optical fiber reduces the risk of a surgeon perceiving a gap between the center of his view and the direction of the laser beam.

Figure 4(a) shows the telescope section of a composite-type optical fiber. The telescope to relay images from the inner surface to the edge of the optical fiber, consisted of quartz lenses in a stainless steel sleeve. The fiber was made of synthetic quartz with three cylindrical structures. Each structure has its own function. A 0.2-mm-diameter center fiber delivered the processing high-energy laser beam. Image fibers to deliver the visible image for the endoscope surrounded the center fiber. The picture elements of the endoscope were laid parallel like a honeycomb and were able to send images from one end to another. There were 20,000 image fibers, so the processing images were transmitted with high clarity and resolution. Light guide fibers to supply illumination intensity were located on the outer side of the image fibers. The total length of the composite-type optical fiber was 10 m. Figure 4(b) shows a view of 0.15 mm mesh through the telescope.

The composite-type optical fiberscope had been originally developed for inspecting and repairing the robot system for tritium breeder blankets in an ITER project. It was improved for application as a surgical device for low infestation treatment[8].

3.2 Laser processing head

The laser processing head was specifically designed to access the inner walls of heat exchanger tubes. It comprised a movable sleeve to be driven by two pulse motors. Both rotational and longitudinal motion were possible on the sleeve to have a 45° tilted mirror at the inside end and an oval hole where a high-energy laser beam and images were transmitted.

Figure 5 is a photograph of the laser processing head inserted in a 1-inch acrylic pipe. The outer diameter was designed to be less than 20 mm. The movable sleeve was supported by ball bearings in a housing, which made it possible to move the processing head 5 mm in the longitudinal direction and rotate it by ±185°.

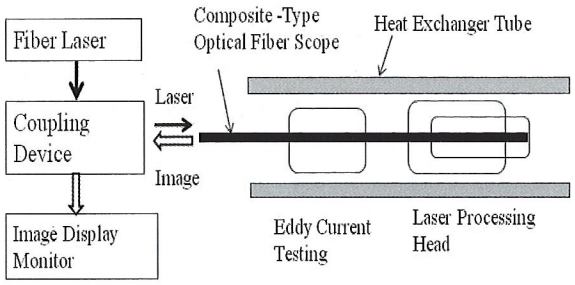

Fig. 3 Schematic view of the prototype probing system

(a) (b)

Fig. 4 Composite-type optical fiber
(a) telescope section, (b) image view of 0.15 mm mesh

3.3 ECT sensor and measurement system

ECT is now widely used in many manufacturing and service environments that require inspection of thin metal for safety-related problems. In the nuclear engineering industry, ECT can be used for certain metal thickness measurements to determine the existence of cracks in metal sheets and tubing. ECT has several advantages over ultrasonic transducer testing. For example, ECT can examine large areas very quickly and it does not require coupling liquids between the sensor and the specimens. Since hundreds of heat exchanger tubes in the heat exchanger units of nuclear power plants require inspection, it is very important to reduce the time of each examination.

Figure 6 is a photograph of the ECT sensor units. To increase the resolution and penetration of this ECT probe system, both a center coil and a pair of induction coils were prepared. The multiple detection coils were placed close to the inner wall of the center unit. Here, 20 detection coils were molded in a plastic hollow mount. One channel consisted of a pair of coils so that 10 channels were applied. When a crack in the inner wall disturbs the eddy current circulation, the magnetic coupling with the detection coils is changed and a defect signal can be read by coil impedance variation. The detection signals were amplified by lock-in amplifiers and were transferred to analog/digital (A/D) converters. In addition, the pair of induction coils induced an intense eddy current with low frequency. The use of the center coil and the induction coils is called remote field. Here it was provided for detecting cracks in the outer side of the heat exchanger tubes.

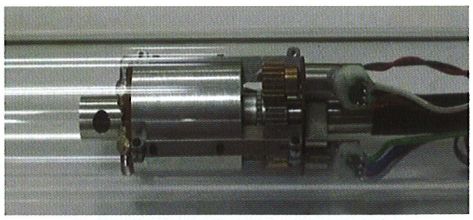

Fig. 5 Laser processing head

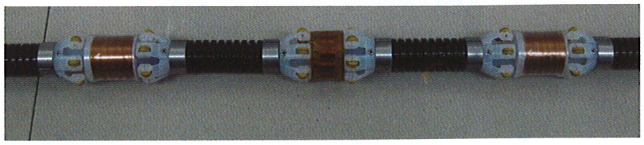

Fig. 6 ECT sensor units

3.4 Coupling device

The function of the coupling device is to axially combine the processing laser beam and the images of the inner tube walls. Figure 7 shows the inside view of the coupling device housing. A laser beam supplied with a quartz block connector for high power coupling (QBH) went into a beam collimator. The collimator was specifically designed for the NA value of the laser beam. A dielectric coating mirror at a 45° angle reflected the 1.07-μm collimated laser beam to a focusing lens. At the end of the composite-type optical fiber, the collimated laser beam was focused on its center core fiber at a 0.2-mm diameter. Visible light coming from the composite-type optical fiber along the opposite direction of the collimated laser beam passed through the dielectric coating mirror to a charge-coupled device (CCD) camera. Reflection loss on the optical components in the coupling device was designed to be less than 10%. Temperature rise was monitored by thermocouples. The housing of the coupling device was sealed and the micro particle density was monitored.

4. Results and discussion

4.1 Laser ablation and peening

A milled surface has a hardened thin layer with residual tensile stress, which is sensitive to SCC susceptibility. Ultrashort laser ablation was useful to remove the hardened thin layer and were applied for mitigation against SCC. However, the improvement of internal residual stress was not been clarified. In the present study, stress measurements have been performed on the laser ablation samples. The synchrotron radiation X-ray in BL22XU at SPring-8 was applied[9]. The energy of the X-ray was 66.84 keV to be able to detect internal residual stress distribution. The stress distribution from the surface to the depth of 0.15 mm was observed using a strain scanning method with a Ge (111) analyzer[10].

Figure 8 shows the depth distribution of residual stress. The surface to the depth of 0.05 mm had high tensile residual stress. The improvement for residual stress was not significantly effective, as shown in the plots of No. 2 and No. 5. However, the improvement for residual stress becomes effective in the plots of No. 8 and No. 9. For No. 2 and No. 5, the laser spot diameter was equal to or less than the trace spacing of 0.6 mm or the shift of 1 mm. The residual stress distribution was improved at the laser spot diameter of 0.9 mm at No. 8. Further improvement was achieved as the number of scanning cycles reached 7 at No. 9. It shows the compressive residual stress condition at the depth of approximately 0.05–0.07 mm. Most of the hardened layers were ablated by ultrashort laser irradiation. During free expansion, the solid density plasma compressed the target on the order of tens of GPa. The intense pressure had been reported by the microscopic observation where the high pressure with ultrashort time duration enabled the generation of intense shockwaves and froze the iron phase in the nonequilibrium state[11]. For laser peening in industrial applications, frequency doubling Q-switched YAG laser pulses in water have been commonly used. It seems that the ultrashort laser ablation has similar effects even in dry condition.

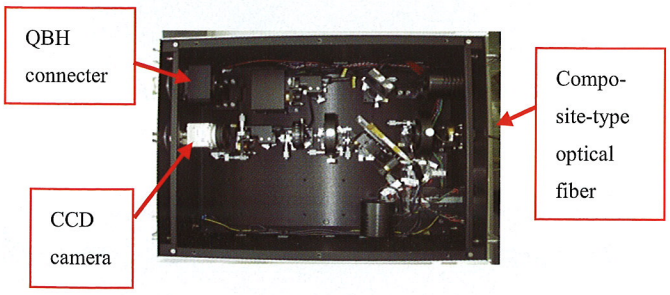

Fig. 7 Inside view of the coupling device housing

4.2 Crack detection

The ECT method was improved to survey the heat exchanger units of FBR "Monju" which has three independent cooling loops within the heat exchanger units. At the present time, there are no defects or cracks on the heat exchanger tubes of any of the loops. Careful inspection will continue into the future. The following paragraph refers to ECT performance using an artificial crack.

Figure 9 shows a crack detection result by the ECT sensor unit. The crack had 0.5 mm wide with a 10% tube thickness, which demonstrates the initial stage of erosion and corrosion. ECT signals from a 10-channel A/D convertor created an original waveform. Noise filters were applied to the original signal. A low pass filter reduced spiky noise and a band cut filter suppressed the periodic pattern in space. A band cut filter successfully extracted the artificial crack, as indicated by the red color in Fig. 9(a). The periodic pattern, the yellow color, was suppressed, which was supposed to indicate the initial deformation on the heat exchanger tube. Generally speaking, the hot rolling process sometimes causes slight deformation. The software also has a function to indicate stereoscopic effect, which is shown in

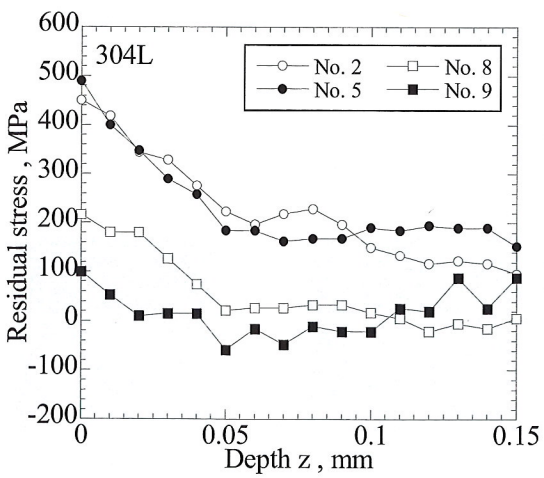

Fig. 8 Depth distribution of residual stress

Fig. 9(b).

4.3 Heating source for welding and its required power

High-energy electron beams have been used for melting, welding, and vaporization in nuclear energy research. For example, in Atomic Vapor Laser Isotope Separation, a high-energy electron beam successfully evaporated uranium or gadolinium metal, which had been charged in a water-cooled crucible[12]. In nuclear fusion research, plasma disruption on a diverter of JT-60 was also demonstrated by electron beam heating[13]. On the other hand, several type lasers have been used for laser welding. Recently, compact fiber lasers have been available for various material welding. They can produce high-focused intensity with a good beam profile on targets in air close to electron beam heating, which will expand the application of the laser welding[14]. In the present work, a compact rare earth element doped fiber laser was chosen for welding.

Here, we have discussed to estimate the required laser power from practical view points. In-process monitoring and adaptive control in continuous wave laser welding was studied by a fiber laser[15]. A 100 W fiber laser carried out micro bead-on-plate welding on 0.1 mm thick stainless steel sheets on an aluminum heat sink. The bead width was 320 μm on the average 10 mm/sec welding speed. It seems that this micro welding scale is similar to that by the probe system. Figure 10 shows a laser welding demonstration by a high power fiber laser. An ytterbium fiber laser and the composite-type optical fiberscope were connected in the coupling device. The laser power was increased to 1 kW. The target was a STBA24 tube containing 2.25% Cr. The working distance from the fiberscope to the target was 19 mm. A shielding glass plate was set to protect the fiberscope lens. Laser power of 300 W with 1 second irradiation had sufficient

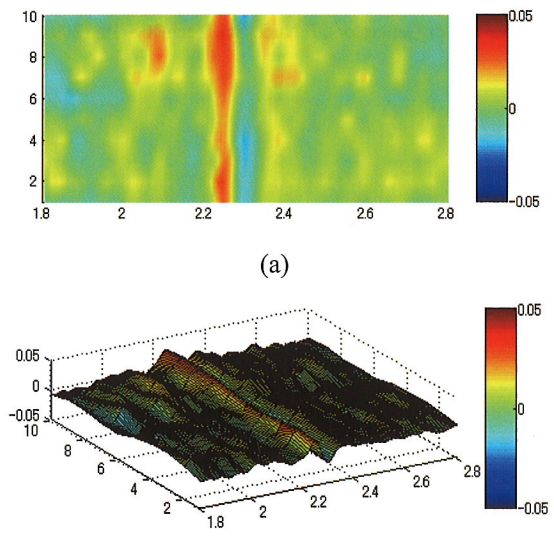

Fig. 9 ECT detection for 1 inch diameter tube
(a) noise filtered signal, (b) stereoscopic view

Here, we have discussed to estimate the required laser power from practical view points. In-process monitoring and adaptive control in continuous wave laser welding was studied by a fiber laser[15]. A 100 W fiber laser carried out micro bead-on-plate welding on 0.1 mm thick stainless steel sheets on an aluminum heat sink. The bead width was 320 μm on the average 10 mm/sec welding speed. It seems that this micro welding scale is similar to that by the probe system. Figure 10 shows a laser welding demonstration by a high power fiber laser. An ytterbium fiber laser and the composite-type optical fiberscope were connected in the coupling device. The laser power was increased to 1 kW. The target was a STBA24 tube containing 2.25% Cr. The working distance from the fiberscope to the target was 19 mm. A shielding glass plate was set to protect the fiberscope lens. Laser power of 300 W with 1 second irradiation had sufficient heat-load for spot welding. The target surface had a shallow dimple of 0.52 mm in diameter and a surrounding molten zone with a diameter of 0.87 mm. Oxide particles were deposited up to a diameter of 1.5 mm. As the laser power was increased over 400 W, surface evaporation and fume generation at the molten pool became strong. Contamination on the shielding glass plate prevented a laser power of over 400 W from reaching the target surface. Therefore, we have determined that a high brilliant fiber laser of 300 W is satisfactory for spot laser welding. The bead-on–plate laser welding on the inside wall of heat exchanger tubes can be planned by the compact 300W ytterbium fiber laser.

Some of Japan's oldest nuclear power plants are now entering their 30th year. To extend their designed lifespan up to 60 years, in-situ flaw sizing and repairs are needed[16]. Careful attention should be required for material degradation caused by water corrosion and radiation damage. The composite-type optical fiber scope combined with laser processing can be treat micro cracks at welded section of heat exchanger tubes.

5. Conclusion

A new probe system was proposed to maintain FBR heat exchanger tubes. Ultrashort pulse laser ablation was applied to the shroud material. Work-hardened layers of 1 × 10 cm SUS304 were successfully removed with reduction of tensile stress.

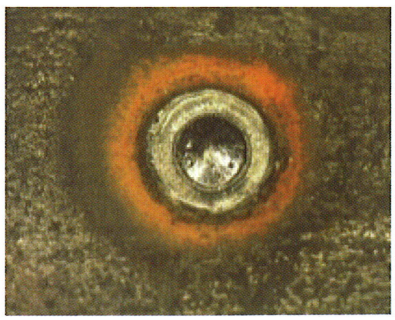

Fig. 10 Molten pool on a heat exchanger tube

A composite-type optical fiberscope was used as the backbone of the newly proposed probe system. ECT units, a laser processing head, and a coupling device were combined in the system. ECT clarified the size of the cracks for repair. A laser welding demonstration decided the laser power of the fiber laser. This system will be tested at the mockup facility for heat exchanger units. This new probe system will demonstrate laser peening for the laser-welded sections of heat exchanger tubes.

Acknowledgments

The authors wish to thank Mr. Tomohiro Akatsu and Mr. Takeshi Seki for their technical assistance. The authors also wish to thank Dr. Takashi Tsukada for his valuable discussion about SCC in the boiling water reactor. And Dr. Toyoaki Kimura, Dr. Atsushi Yokoyama and Dr. Shunichi Kawanishi kindly gave the authors their continuous support in promoting this project.

The present study includes the results of "Development of maintenance technologies with a new probe system for FBR heat exchanger tubes" entrusted to the Japan Atomic Energy Agency by the Ministry of Education, Culture, Sports, Science and Technology of Japan (MEXT).

References

1) Kutsuna, M.: Fundamental of Laser Welding, J. Jpn Laser Processing Soc., **15**-4, (2003), 210.
2) Oka, K., Itou, A. and Takiguchi, Y.: Development of Bore Tools for Pipe Welding and Cutting, J. Robotics and Mechatronics, **10**-2, (1998), 104.
3) Oka, K., Tada, E., Kimura, S., Ogawa, T. and Sasaki, N.: Development of In-pipe Access Welding and Cutting Tool using YAG Laser, SPIE Proc., **3888**, (1999), 702.
4) Sano, Y., Kimura, M., Yoda, M., MUkai, N., Sato, K., Uehara, T., Ito, T., Shimamura, M., Sudo, A. and Suezono, N.: Development of Fiber-Delivered Laser Peening System to Prevent Stress Corrosion Cracking of Reactor Components, Proc. 9th Int. Conf. on Nuclear Engineering (ICONE-9), France, (2001), RefNum. 33008009.
5) Nishimura, A., Minehara, E., Tsukada, T., Kikuchi, M. and Nakano, J.: Ablation of Work Hardening Layers against Stress Corrosion Cracking of Stainless Steel by Repetitive Femtosecond Laser Pulses, SPIE Proc., **5562**, (2004), 673.
6) McMaster R.C. ed.: Nondestructive Testing Handbook, 2nd ed., Vol. 4, Electromagnetic Testing, American Society for Nondestructive Testing, (1986), 26.
7) Inoue, T., Sueoka, A., Nakano, Y., Kanemoto, H., Imai Y. and Yamaguchi, T.: Vibration of Probe Used for the Defect Detection of Helical Heating Tubes in a Fast Breeder Reactor, Part 1 Experimental Results by Using Mock-UP, Nucl. Eng. Design, **237**, (2007), 858.
8) Oka, K., Aganawa, A., Yamashita, H., Nakamura. T. and Chiba, T.: Composite-Type Optical Fiberscope for Laser Surgery for Twin-to-Twin Transfusion Syndrome, Medical Imaging and Augmented Reality, **5128**, (2008), 251.
9) Shobu, T., Tozawa, K., Shiwaku, H., Konishi, H., Inami, T., Harami, T. and Mizuki, J.:Wide Band Energy Beamline Using Si(111) Crystal Monochromators at BL22XU in Spring-8, AIP Conf. Proc. **879**, (2007), 902.
10) Shobu, T., Mizuki, J., Suzuki, K., Akiniwa, Y. and Tanaka, K. : High Space-Resolitive Evaluation of Subsurface Stress Distribution by Strain Scanning Method with Analyzer Using High-Energy Synchrotron X-rays, JSME Int. J., Ser. A, **49**-3, (2006), 376.
11) Sano, T., Mori, H., Ohnuma, E. and Miyamoto, I.: Femtosecond Laser Quenching of the ε Phase of Iron, Appl. Phys. Lett., **83**-17, (2003), 3498.
12) Nishimura, A., Ohba, H., Ogura K. and Shibata, T.: Measurement of the Absolute Ocillator Strengths of Gadolinium using an Atomic Vapor Produced by Electron Beam Heating, Opt. Commun., **110**, (1994), 561.
13) Nakamura, K., Suzuki, S., Dairaku, M., Yokoyama, K., Okumura, Y., Suzuki, T., Jimbo, Bandourko, V. and Akiba, M.: Disruption and Sputtering Erosions on SiC doped CFC, J. Nucl. Mat., **258**, (1998), 828.
14) Kawahito, Y., Matsumoto, N., Mizutani. N., Katayama. S.: Characterisation of Plasma Induced during High Power Fibre Laser Welding of Stainless Steel, Sci. Tech. Weld. Join., **13**-8, (2008), 744.
15) Kawahito, Y., Kawasaki, M. and Katayama, S: In-process Monitoring and Adaptive Control during Micro Welding with CW Fiber Laser, J. Laser Micro Nano Eng., **3**-1, (2007), 46.
16) Yamashita,Y.: Newly Undertaken Inspection and Repairs for Aged Nuclear Power Generators, J. Nucl. Sci. Tech., **38**-10, (2001), 887.